

Green synthesis of a magnetite/graphitic carbon nitride 2D nanocomposite for efficient Hg²⁺ remediation

Raghuraj Singh Chouhan,^{a*} Jan Gačnik^a, Igor Živković^a, Sreekanth Vijayakumaran Nair^{a,b}, Nigel Van de Velde^c, Alenka Vesel^d, Primož Šket^e, Sonu Gandhi^{f*}, Ivan Jerman^{c*}, Milena Horvat^{a*}

^aDepartment of Environmental Sciences, Jožef Stefan Institute, Jamova Cesta 39, 1000 Ljubljana, Slovenia.

^bJožef Stefan International Postgraduate School, Jamova Cesta 39, 1000 Ljubljana, Slovenia.

^cNational Institute of Chemistry, Hajdrihova 19, 1000 Ljubljana, Slovenia

^dDepartment of Surface Engineering, Jožef Stefan Institute, Jamova 39, 1000 Ljubljana, Slovenia

^eSlovenian NMR Center, National Institute of Chemistry, Hajdrihova 19, 1000 Ljubljana, Slovenia

^fDBT-National Institute of Animal Biotechnology (DBT-NIAB), Hyderabad, Telangana 500032, India.

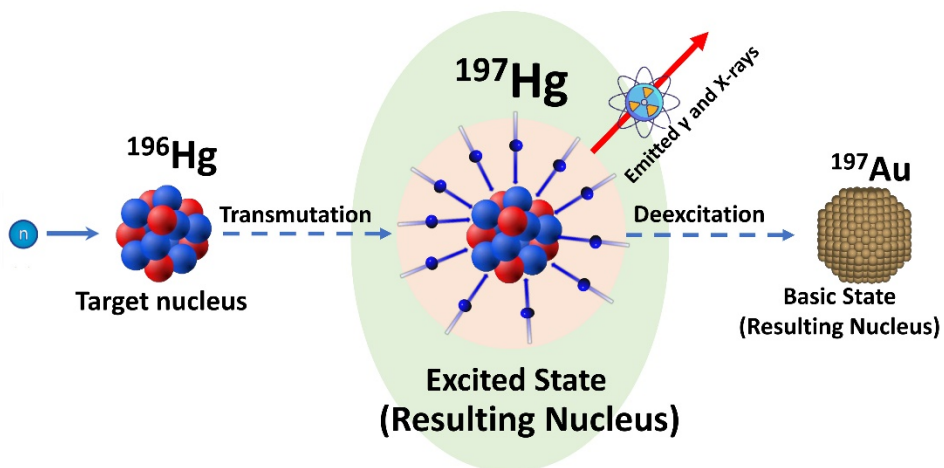


Fig. S1. A schematic representation of the reaction mechanism for generating ^{197}Hg radiotracer.

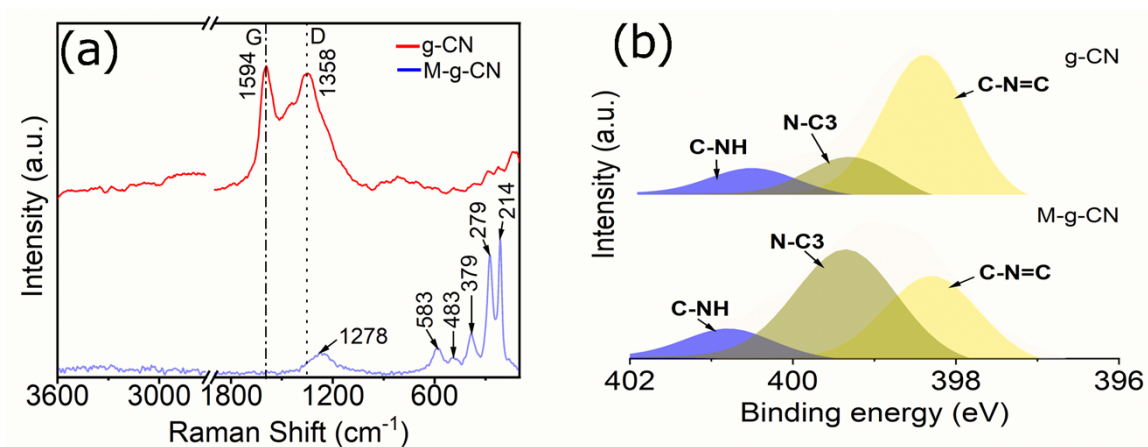


Fig. S2 (a) Raman, and (b) N1 XPS profile of g-CN and M-g-CN

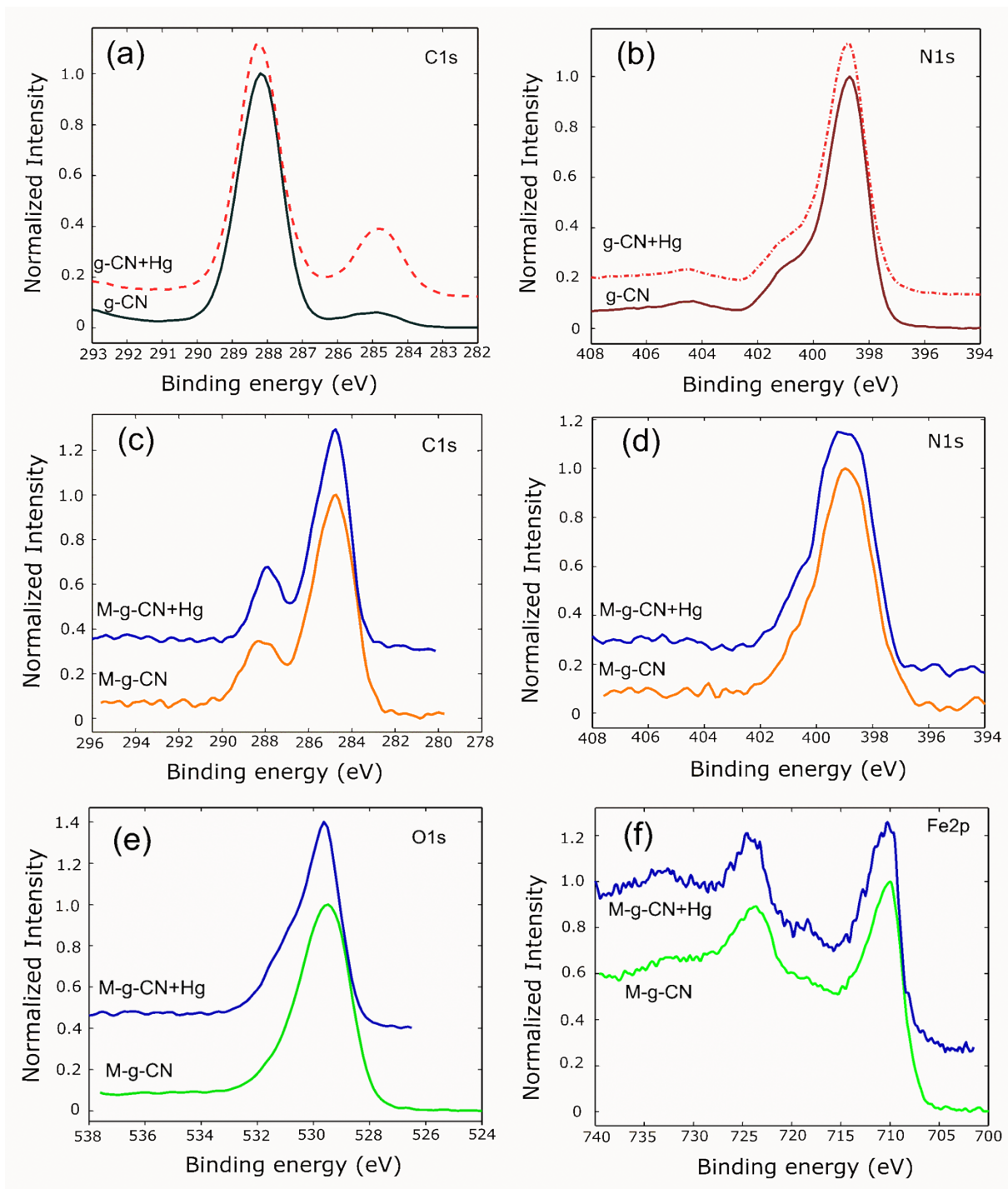


Fig S3. XPS spectra of as-prepared samples. **(a,b)** C1s and N1s of g-CN with and without Hg^{2+} . **(c,d)** M-g-CN with and without Hg^{2+} . **(e,f)** O1s spectra and Fe2p survey spectra of both samples.

Table S1. Surface elemental arrangement of the samples in at.% calculated from survey spectra (**Fig S3f.**)

Sample	C	N	O	Na	Fe	Hg	Cl
Without Hg ²⁺	24.3	6.4	51.5	3.0	14.9		
With Hg ²⁺	46.0	12.8	30.9	0.5	8.0	0.5	1.4

1. Analysis of samples using CP-MAS-NMR

The coordination of ions in g-CN+Hg²⁺ was demonstrated using ¹³C and ¹⁵N CP-MAS NMR spectra of g-CN and g-CN+Hg²⁺. The ¹³C CP-MAS NMR spectrum of g-CN showed two groups of signals (Fig S4). The low-field signals between δ 160 and 170 ppm corresponded to carbon atoms adjacent to the amino groups (Fig S6, 1). The signals observed for carbon atoms marked (Fig S6, 2) resonated between δ 152 and 160 ppm. In the ¹⁵N CP-MAS NMR spectrum of g-CN, a signal at δ -245 ppm was observed, which belonged to the bridging nitrogen atom marked (Fig S6, 5), while the outer ring nitrogen atoms (Fig S6, 4) resonated between δ -170 and -210 ppm (Fig S5a). The signals for amino nitrogen atoms (Fig S6, 3) appeared between δ -260 and -285 ppm (Fig S5a). Changes in the shape and chemical shifts of signals in the ¹³C and ¹⁵N CP-MAS NMR spectra, particularly for the outer ring nitrogen atoms between δ -170 and -210 ppm, were observed after salt soaking, indicating the coordination of Hg cations with the heptazine rings of g-CN (Figs S4 and S5b). Similar changes in ¹³C and ¹⁵N CP-MAS NMR spectra have been previously observed in g-CN soaked with KCl.¹

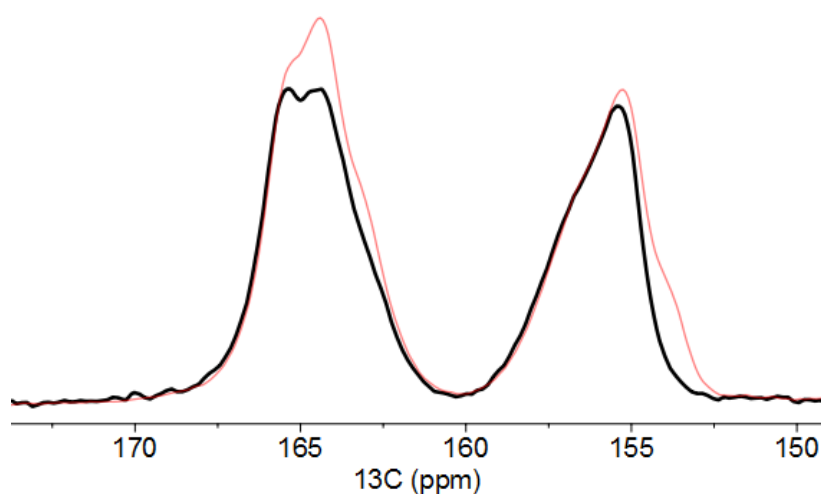


Fig S4 ¹³C CP-MAS of g-CN (black) and g-CN+ Hg²⁺ (red). The observed variations in signal shape and chemical shifts among the spectra indicate an interaction between Hg²⁺ and g-CN. Chemical shifts were referenced to tetramethylsilane. The spectra were obtained using a 600 MHz NMR spectrometer with a spinning rate of 16 kHz.

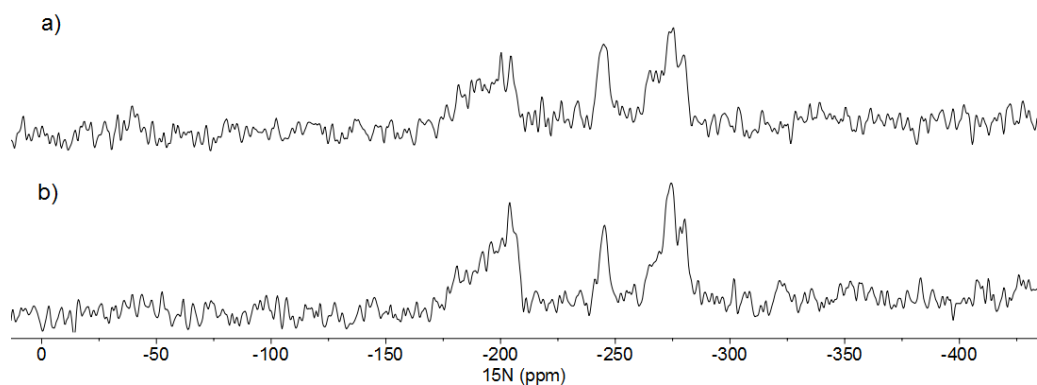


Fig S5. ^{15}N CP-MAS of g-CN (a) and g-CN+ Hg^{2+} (b). A significant difference is noticeable in the signals attributed to the outer ring nitrogen atoms marked with 4 in Fig S6, resonating between δ -170 and -210 ppm, suggesting the coordination of Hg cations with the heptazine rings of g-CN. Chemical shifts were referenced to nitromethane. The spectra were obtained using a 600 MHz NMR spectrometer with a spinning rate of 10 kHz.

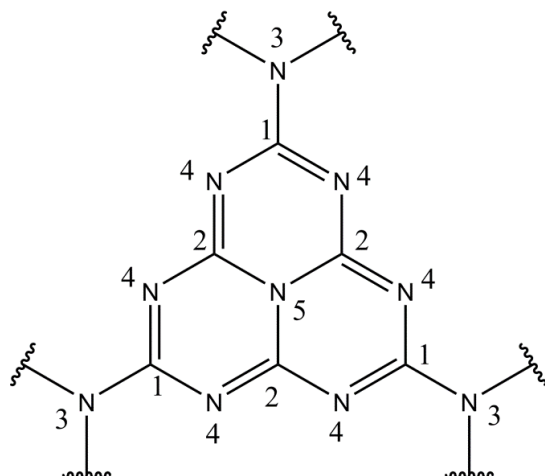


Fig S6. Heptazine core with atom numbering.

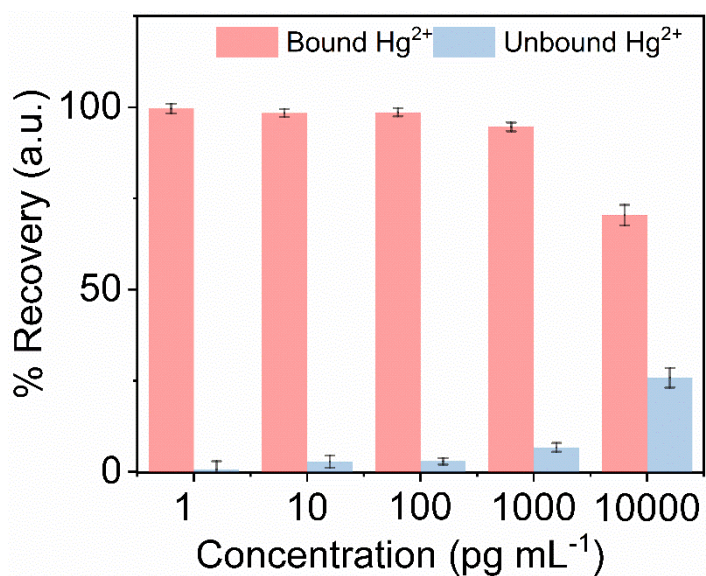


Fig S7. Binding efficiency of M-g-CN with different concentrations of Hg^{2+} .

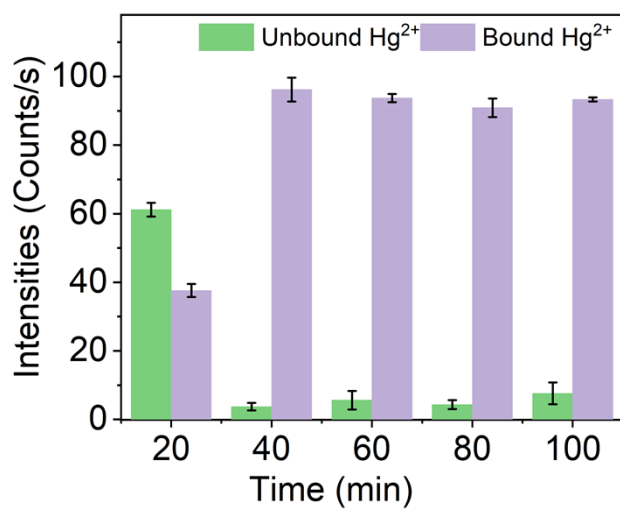


Fig S8. Amount of time required by M-g-CN to bind Hg^{2+} in the solution.

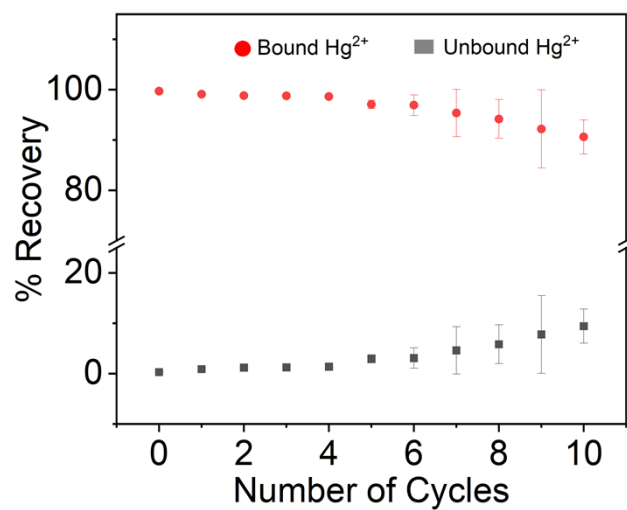


Fig S9. Reusability studies of as synthesized M-g-CN with repeated cycles of Hg^{2+} binding.

Table S2. Maximum binding efficiency of M-g-CN with different concentrations of Hg²⁺

Amount of Material (mg mL ⁻¹)	Trials	Concentration of Hg ²⁺ (pg mL ⁻¹)	Recoveries of Hg ²⁺ expressed as % of the spiked Hg ²⁺ concentration			
			Hg ²⁺ adsorbed on the material (M-g-CN)		Hg ²⁺ remains in the solution (Unbound)	
			Bound Hg ²⁺	Average (± SD) of bound Hg ²⁺	Unbound Hg ²⁺	Average (± SD) of unbound Hg ²⁺
100	I	1	99.65	99.35 (± 0.35)	0.71	0.97 (± 0.36)
	II	1	99.12		1.23	
100	I	10	98.99	98.18 (± 1.14)	2.83	2.16 (± 0.94)
	II	10	97.37		1.49	
100	I	100	98.99	98.84 (± 0.20)	2.29	2.45 (± 0.07)
	II	100	98.71		2.62	
100	I	1000	95.88	94.99 (± 1.25)	6.76	6.2 (± 0.70)
	II	1000	94.11		5.77	
100	I	10000	71.05	70.91 (± 0.19)	24.45	25.18 (± 1.03)
	II	10000	70.77		25.91	

Table S3. Real matrices recovery studies

Matrices	Trials	Spiked Hg ²⁺ (pg mL ⁻¹)	Recoveries of Hg ²⁺ expressed as % of the spiked Hg concentration			
			Hg ²⁺ adsorbed on the material (M-g-CN)		Hg ²⁺ remains in the solution (Unbound)	
			Bound Hg ²⁺	Average (± SD) of bound Hg ²⁺	Unbound Hg ²⁺	Average (± SD) of unbound Hg ²⁺
Marine	I	50	96.7	96.0 (± 1.08)	4.55	4.53 (± 0.03)
	II	50	95.2		4.51	
Stream	I	50	98.0	97.5 (± 0.61)	3.22	3.56 (± 0.49)
	II	50	97.1		3.29	
Precipitation	I	50	98.6	98.2 (± 0.44)	2.89	2.69 (± 0.28)
	II	50	97.9		2.50	
Ultra-pure	I	50	99.8	99.4 (± 0.57)	0.19	0.14 (± 0.06)
	II	50	99.0		0.10	

Table S4. Interference studies

Interfering Ions	Ions Concentration (µg mL ⁻¹) Natural Environment	Hg ²⁺ Concentration (pg mL ⁻¹)	Trials	Recoveries of Hg ²⁺ expressed as % of the spiked Hg ²⁺ concentration			
				Hg ²⁺ adsorbed on the material (M-g-CN)		Hg ²⁺ remains in the solution (Unbound)	
				Bound Hg ²⁺	Average (± SD) of bound Hg ²⁺	Unbound Hg ²⁺	Average (± SD) of unbound Hg ²⁺
Na ⁺ Marine	11000	50	I	99.78	99.38 (± 0.55)	1.69	1.40 (± 0.40)
	11000	50	II	98.99		1.12	
Na ⁺ Stream	10	50	I	98.71	97.78 (± 1.30)	3.84	3.11 (± 1.32)
	10	50	II	96.86		2.39	
K ⁺	200	50	I	98.66	98.83 (± 0.24)	1.39	2.19 (± 1.13)
	200	50	II	99.01		2.99	
Ca ⁺	400	50	I	99.54	100.05 (± 0.65)	0.95	1.25 (± 0.43)
	400	50	II	100.47		1.56	
Ag ⁺	0.002	50	I	97.11	97.56 (± 0.64)	3.53	3.22 (± 0.44)
	0.002	50	II	98.02		2.92	
Co ²⁺	0.01	50	I	99.32	99.77 (± 0.63)	1.81	1.39 (± 0.58)
	0.01	50	II	100.22		0.98	

Zn ²⁺	10	50	I	97.99	98.33 (± 0.48)	3.93	3.34 (± 0.83)
	10	50	II	98.67		2.75	
Fe ³⁺	0.03	50	I	95.94	97.23 (± 1.83)	3.63	4.13 (± 0.70)
	0.03	50	II	98.53		4.63	
Mn ²⁺	0.2	50	I	100.11	99.55 (± 0.63)	0.59	0.74 (± 0.21)
	0.2	50	II	99.1		0.95	
Ni ²⁺	0.002	50	I	99.88	99.57 (± 0.43)	0.06	0.42 (± 0.50)
	0.002	50	II	99.27		0.78	
Bi ³⁺	1x10 ⁻⁵	50	I	98.99	98.01 (± 1.40)	2.62	3.16 (± 0.77)
	1x10 ⁻⁵	50	II	97.01		3.71	
Cl ⁻	35000	50	I	99.7	99.88 (± 0.26)	0.66	0.49 (± 0.23)
	35000	50	II	100.07		0.33	
Br ⁻	70	50	I	99.71	99.35 (± 0.50)	1.82	1.77 (± 0.07)
	70	50	II	99.43		1.72	
I ⁻	1	50	I	96.27	97.42 (± 1.62)	4.71	3.76 (± 1.34)
	1	50	II	98.57		2.81	

Table S5. Reusability studies

No. of Reusable Cycles	Trials	Concentration of Hg ²⁺ (pg mL ⁻¹)	Recoveries of Hg ²⁺ expressed as % of the spiked Hg ²⁺ concentration			
			Hg ²⁺ adsorbed on the material (M-g-CN)		Hg ²⁺ remains in the solution (Unbound)	
			Bound Hg ²⁺	Average (± SD) of bound Hg ²⁺	Unbound Hg ²⁺	Average (± SD) of unbound Hg ²⁺
0	I	100	99.66	99.70 (± 0.06)	0.34	0.29 (± 0.06)
	II	100	99.75		0.25	
1	I	100	98.92	99.14 (± 0.31)	0.18	0.80 (± 0.87)
	II	100	99.37		1.42	
2	I	100	98.85	98.81 (± 0.04)	1.43	1.38 (± 0.07)
	II	100	98.78		1.32	
3	I	100	98.77	98.75 (± 0.02)	1.23	1.19 (± 0.05)
	II	100	98.73		1.15	
4	I	100	98.24	98.60 (± 0.50)	1.76	1.40 (± 0.50)
	II	100	98.96		1.04	
5	I	100	96.93	97.06 (± 0.19)	3.10	2.83 (± 0.38)
	II	100	97.20		2.55	
6	I	100	96.85	96.91 (± 0.09)	2.36	2.94 (± 0.81)
	II	100	96.98		3.52	
7	I	100	95.11	95.36 (± 0.36)	1.66	3.10 (± 2.03)
	II	100	95.62		4.54	
8	I	100	95.36	94.17 (± 1.67)	5.80	5.43 (± 0.55)
	II	100	92.99		5.03	
9	I	100	92.10	92.18 (± 0.12)	13.3	7.79 (± 7.72)
	II	100	92.27		2.33	
10	I	100	90.06	90.58 (± 0.74)	7.92	8.11 (± 0.25)
	II	100	91.11		8.29	

Reference:

- 1 H. Gao, S. Yan, J. Wang and Z. Zou, *Dalt. Trans.*, 2014, **43**, 8178–8183.